

**Science**

 AAAS

**Trojan Horse Strategy in Agrobacterium  
Transformation: Abusing MAPK Defense Signaling**

Armin Djamei, *et al.*  
*Science* **318**, 453 (2007);  
DOI: 10.1126/science.1148110

***The following resources related to this article are available online at  
www.sciencemag.org (this information is current as of November 5, 2007 ):***

**Updated information and services**, including high-resolution figures, can be found in the online version of this article at:

<http://www.sciencemag.org/cgi/content/full/318/5849/453>

**Supporting Online Material** can be found at:

<http://www.sciencemag.org/cgi/content/full/318/5849/453/DC1>

This article **cites 14 articles**, 5 of which can be accessed for free:

<http://www.sciencemag.org/cgi/content/full/318/5849/453#otherarticles>

This article appears in the following **subject collections**:

Botany

<http://www.sciencemag.org/cgi/collection/botany>

Information about obtaining **reprints** of this article or about obtaining **permission to reproduce this article** in whole or in part can be found at:

<http://www.sciencemag.org/about/permissions.dtl>

mitochondrial small subunit (SSU) ribosomal RNA (rRNA) (15) and a bacterial transfer messenger RNA (tmRNA) (16) that function in a two-piece form, in contrast to the *C. merolae* tRNAs reported here that function in a one-piece form. The permuted rRNA and tmRNA genes are hypothesized to have arisen by a gene duplication that formed a tandem repeat, followed by the loss of the outer segment of each copy (15, 17). Even if a circular permutation occurred in tRNA genes, most of the resulting permuted genes would not be retained in the genome because of the failure of expression or the loss of functional structure of the RNA. In *C. merolae*, however, permuted tRNA genes might have persisted in the genome because of the use of the upstream promoter by the transcription system and processing of the circularly permuted pre-tRNA into a canonical tRNA molecule by the tRNA-splicing machinery. Considering that *C. merolae* is an early rooted eukaryote and that the BHB motifs would play a pivotal role in the tRNA processing, it is possible that the permuted

tRNA genes might have developed via a common process with the split-tRNA genes of *Nanoarchaeum equitans* (18). Further investigation should provide a hint about how to evaluate the evolution of tRNA genes in the early eukaryote.

#### References and Notes

1. T. Kuroiwa, *Bioessays* **20**, 344 (1998).
2. M. Matsuzaki *et al.*, *Nature* **428**, 653 (2004).
3. H. Nozaki *et al.*, *J. Mol. Evol.* **56**, 485 (2003).
4. T. M. Lowe, S. R. Eddy, *Nucleic Acids Res.* **25**, 955 (1997).
5. Materials and methods are available on Science Online.
6. J. Sugahara *et al.*, *In Silico Biol.* **6**, 411 (2006).
7. J. Sugahara, N. Yachie, K. Arakawa, M. Tomita, *RNA* **13**, 671 (2007).
8. T. Pan, O. C. Uhlenbeck, *Gene* **125**, 111 (1993).
9. G. Galli, H. Hofstetter, M. L. Birnstiel, *Nature* **294**, 626 (1981).
10. M. Hamada, A. L. Sakulich, S. B. Koduru, R. J. Maraia, *J. Biol. Chem.* **275**, 29076 (2000).
11. J. Abelson, C. R. Trotta, H. Li, *J. Biol. Chem.* **273**, 12685 (1998).
12. A. M. Weiner, *Curr. Biol.* **14**, R883 (2004).
13. S. Altman, L. Kirsebom, S. Talbot, *FASEB J.* **7**, 7 (1993).

14. H. Schurer, S. Schiffer, A. Marchfelder, M. Morl, *Biol. Chem.* **382**, 1147 (2001).
15. T. Y. Heinonen, M. N. Schnare, P. G. Young, M. W. Gray, *J. Biol. Chem.* **262**, 2879 (1987).
16. K. C. Keiler, L. Shapiro, K. P. Williams, *Proc. Natl. Acad. Sci. U.S.A.* **97**, 7778 (2000).
17. K. P. Williams, *Nucleic Acids Res.* **30**, 2025 (2002).
18. L. Randau *et al.*, *Nature* **433**, 537 (2005).
19. M. Sprinzl, K. S. Vassilenko, *Nucleic Acids Res.* **33**, D139 (2005).
20. Supported by Japan Society of the Promotion of Science (JSPS) Fellowships (7473 to A.S. and 1924 to N.Y.), by Grants-in-Aid for Creative Scientific Research (17GS0314 to Y.S. and 16GS0304 to F.K.) from JSPS and Ministry of Education, Culture, Sports, Science and Technology, respectively, by grants from the Yamagata Prefectural Government and Tsuruoka City in Japan (to M.T., A.K., J.S., and N.Y.), and by the Frontier project Adaptation and Evolution of Extremophile (to Y.S.).

#### Supporting Online Material

www.sciencemag.org/cgi/content/full/318/5849/450/DC1  
Materials and Methods

Figs. S1 to S5

References and Notes

29 May 2007; accepted 31 August 2007

10.1126/science.1145718

## Trojan Horse Strategy in *Agrobacterium* Transformation: Abusing MAPK Defense Signaling

Armin Djamei,<sup>1\*†</sup> Andrea Pitzschke,<sup>1†</sup> Hirofumi Nakagami,<sup>1†‡</sup> Iva Rajh,<sup>1</sup> Heribert Hirt<sup>1,2</sup>

Nuclear import of transfer DNA (T-DNA) is a central event in *Agrobacterium* transformation of plant cells and is thought to occur by the hijacking of certain host cell proteins. The T-DNA-associated virulence protein VirE2 mediates this process by binding to the nuclear import machinery via the host cell factor VIP1, whose role in plants has been so far unknown. Here we show that VIP1 is a transcription factor that is a direct target of the *Agrobacterium*-induced mitogen-activated protein kinase (MAPK) MPK3. Upon phosphorylation by MPK3, VIP1 relocates from the cytoplasm to the nucleus and regulates the expression of the *PR1* pathogenesis-related gene. MAPK-dependent phosphorylation of VIP1 is necessary for VIP1-mediated *Agrobacterium* T-DNA transfer, indicating that *Agrobacterium* abuses the MAPK-targeted VIP1 defense signaling pathway for nuclear delivery of the T-DNA complex as a Trojan horse.

Higher eukaryotes recognize microbes through pathogen-associated molecular patterns (PAMPs) and activate the innate immune response in animals and plants (1). The perception of PAMPs leads to rapid activation of host defense mechanisms, including the activation of mitogen-activated protein

kinases (MAPKs), production of reactive oxygen species, and subsequent induction of defense-related genes. However, virulence factors of successful pathogens can inhibit PAMP-elicited basal defenses (2). In specific cases, plants have evolved resistance proteins specialized to detect these pathogen-derived virulence factors or their effects on host targets. As a consequence, a hypersensitive response (HR) occurs that includes localized cell death and the arrest of pathogen spread (3, 4).

*Agrobacterium* transforms plants by transporting a single-stranded copy of the transfer DNA (T-DNA) from its tumor-inducing Ti plasmid into the host cell and integrating it into the host cell genome. The agrobacterial transformation process is mediated by Vir (virulence) proteins. The T-DNA strand that is exported into

plant cells has the VirD2 protein covalently attached to its 5' end. The VirE2 protein, which is translocated into plant cells independently of the T-DNA strand, associates with the T strand in the plant cell (5) before nuclear import mediated by cellular karyopherin  $\alpha$ , which binds to VirD2. Nuclear import is further facilitated by the host protein VIP1, which functions as an adaptor (6), but whose cellular function is as yet unknown.

PAMPs activate a variety of plant MAPK cascades (7), which make a major contribution to the host defense responses. In *Arabidopsis thaliana*, PAMPs such as flagellin activate at least three MAPKs—MPK3, MPK4, and MPK6—resulting in altered expression of various stress-responsive genes (8–10). So far, the direct downstream targets of these plant MAPKs are largely unknown. In this study, we show that *Agrobacterium* triggers the activation of several MAPKs, including MPK3, and we identify VIP1 as a target of MPK3.

A yeast two-hybrid screen was performed in order to find interactors with MPK3. Clones carrying full-length cDNAs of VIP1 (VirE2-interacting protein At1g43700) (11) were repeatedly isolated. The VIP1-MPK3 interaction in yeast was confirmed by its ability to induce another reporter gene, *lacZ*, encoding for  $\beta$ -galactosidase (Fig. 1A). In order to test whether VIP1 also interacts with other MAPKs, targeted yeast two-hybrid interaction experiments were performed with VIP1 and representatives of all the *A. thaliana* MAPK subfamilies (MPK2, -3, -4, -5, -6, -7, -16, and -17). VIP1-MAPK interaction was specific for MPK3, because neither MPK6, the closest homolog of MPK3, nor any of the other MAPKs tested interacted with VIP1 (Fig. 1A).

To substantiate these results, we transiently expressed MPK3 and VIP1 in *Arabidopsis*

<sup>1</sup>Department of Plant Molecular Biology, Max F. Perutz Laboratories, University of Vienna, Dr.-Bohr-Gasse 9, 1030 Vienna, Austria. <sup>2</sup>URGV Plant Genomics Laboratory, 2 Rue Gaston Crémieux, 91057 Evry, France.

\*Present address: Department of Organismic Interactions, Max-Planck-Institut für terrestrische Mikrobiologie, Karl-von-Frisch-Strasse, 35043 Marburg, Germany.

†These authors contributed equally to this work.

‡Present address: Plant Immunity Research Team, RIKEN Plant Science Center, 1-7-22 Suehiro-cho, Tsurumi, Yokohama 230-0045, Japan.

protoplasts under control of the constitutive cauliflower mosaic virus 35S promoter as C-terminally tagged proteins with either hemagglutinin (HA) or Myc epitopes that allowed the immunoprecipitation and immunoblotting of the proteins. From protein extracts of protoplasts expressing MPK3-HA alone (negative control) or coexpressing MPK3-HA and VIP1-Myc, VIP1-Myc was immunoprecipitated using an antibody to Myc. MPK3-HA could be coimmunoprecipitated with VIP1-Myc (Fig. 1B). We also found coimmunoprecipitation of MPK3-HA with VIP1-phosphoderivatives VIP1\_A-Myc and VIP1\_D-Myc, as well as with its known activator MKK4-Myc (8), but not of MPK3-HA when expressed alone (Fig. 1B). These findings support the notion that VIP1 and MPK3 are true interaction partners.

VIP1 contains a single potential MAPK phosphorylation site, Ser<sup>79</sup> (Fig. 1C). To test whether VIP1 can be targeted by MPK3, recombinant glutathione S-transferase (GST) fusion proteins of VIP1, VIP1\_A (Ser<sup>79</sup>→Ala<sup>79</sup>, mimicking constitutively nonphosphorylated VIP1), and VIP1\_D

(Ser<sup>79</sup>→Asp<sup>79</sup>, mimicking constitutively phosphorylated VIP1) were produced. To obtain active MPK3, MPK3-HA was coexpressed in protoplasts with its upstream activator MKK4 and immunoprecipitated using an antibody to HA. When recombinant GST-VIP1 was incubated with immunoprecipitated MPK3-HA in the presence of <sup>32</sup>P-γ-labeled adenosine triphosphate, it became phosphorylated by MPK3, as did the artificial MAPK substrate myelin basic protein (MBP) but not GST (Fig. 1D). We also observed VIP1 phosphorylation by recombinant GST-MPK3 (fig. S1), excluding the possibility that VIP1 might be the substrate of a kinase that had been coimmunoprecipitated with MPK3-HA. Moreover, no signal was detected when the kinase assays were performed with recombinant VIP1 derivatives VIP1\_A or VIP1\_D that, due to mutation of Ser<sup>79</sup>, lack a MAPK phosphorylation site (fig. S1). These results indicate that VIP1 is a substrate of MPK3 and that Ser<sup>79</sup> in VIP1 corresponds to the phosphorylation site in VIP1.

It is thought that most MAPKs are located in the cytoplasm and relocate to the nucleus

after activation, where they phosphorylate transcription factors. In animals, the subcellular localization and thereby the activity of transcription factors can also be controlled through phosphorylation by a MAPK residing in the cytoplasm (12), but whether plant transcription factors can also be regulated in this way is so far unknown. Our results indicate that VIP1 can interact with and be phosphorylated by MPK3 (Fig. 1).

Whether VIP1 phosphorylation could affect its localization was addressed by in vivo confocal microscopy of transgenic *Arabidopsis* plants expressing C-terminally tagged VIP1-YFP fusion protein (YFP, yellow fluorescent protein). To this end, wild-type VIP1 and the mutated versions VIP1\_A and VIP1\_D were expressed under the control of an estradiol-inducible promoter. A minimum of six independent lines of each construct were analyzed. As shown in Fig. 2A, wild-type VIP1-YFP was detected in the cytoplasm and in the nucleus. VIP1\_A-YFP showed a similar localization. In contrast, VIP1\_D-YFP was predominantly nuclear. These results suggest that VIP1 can reside in both the nuclear and the cytoplasmic compartment and that its localization is regulated by the phosphorylation state of Ser<sup>79</sup>. The reason why VIP1\_A-YFP is not exclusively extranuclear and VIP1\_D is not exclusively intranuclear might be due to homomultimerization with endogenous VIP1, because VIP1 has been shown to form homomultimers (13).

To investigate whether MPK3 activation could affect the subcellular localization of VIP1, we treated estradiol-induced VIP1-YFP plants with flg22 peptide corresponding to the highly conserved flagellin sequence of pathogenic bacteria (8). Plants recognize flg22 and initiate a signaling cascade that results in the activation of MPK3 within 5 min (9). Upon treatment with flg22, a strong decrease in the cytoplasmic and a concomitant increase in the nuclear pool of VIP1-YFP was observed (Fig. 2B), whereas VIP1\_A-YFP showed no such relocalization (fig. S2). These results support the notion that MPK3 activity regulates the subcellular localization of VIP1 via the phosphorylation of Ser<sup>79</sup>. Previous studies on VIP1 focused on its role during the transformation of plant cells by agrobacteria (6). Assuming that MPK3 is regulating VIP1 localization by phosphorylation, we then wondered whether MPK3 actually gets activated in plants by agrobacteria, which, unlike most pathogenic bacteria, have a distinct flagellin that is not recognized by the plant flagellin receptor FLS2 that is upstream of MPK3 and MPK6 (8). By in vitro kinase assays using MBP as a substrate, we analyzed the activity of MPK3 in 12-day-old *Arabidopsis* wild-type seedlings at 2, 5, and 10 min after treatment with agrobacteria. We also tested two other PAMP-activated MAPKs, MPK4 and MPK6. As compared to mock-treated seedlings, the activities of MPK3, MPK4, and MPK6 strongly increased upon incubation with the agrobacteria (Fig. 2D). Activation of these MAPKs could already be detected 5 min after

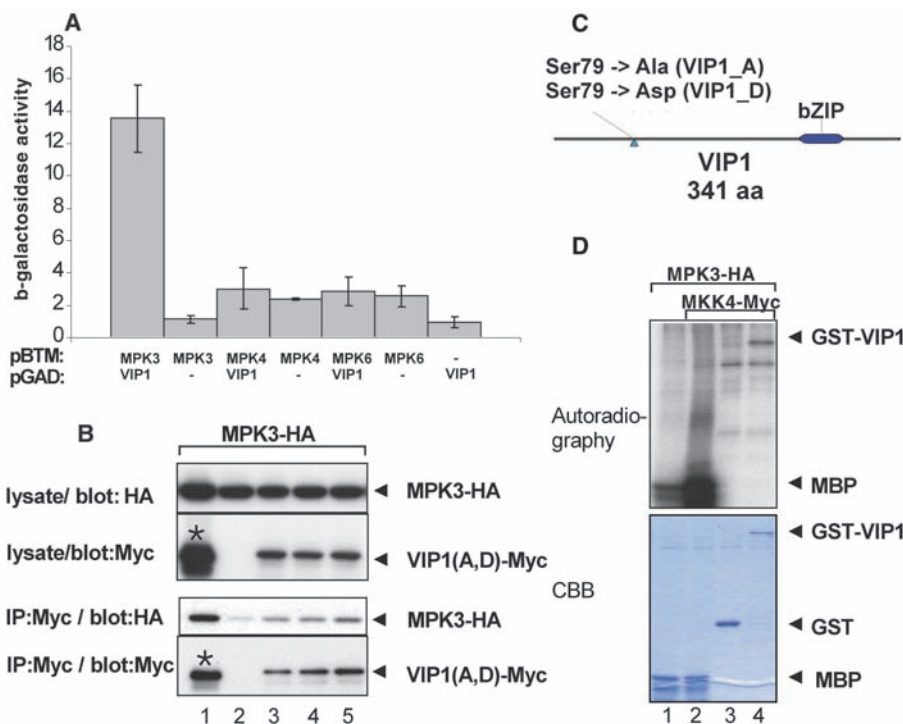


**Fig. 1.** VIP1 interacts with and is phosphorylated by MPK3. **(A)** Yeast two-hybrid analysis. The interaction of VIP1 (fused to activation domain, in pGAD) and MPK3, -4, and -6 (fused to binding domain, in pBTM) and the respective empty vector controls (-) as quantified by β-galactosidase activity assay is shown (*n* = 9 independent yeast cotransformants; error bars indicate SD). **(B)** Coimmunoprecipitation. Protoplasts were transfected with MPK3-HA alone (lane 2) or in combination with Myc-tagged VIP1 (lane 3) or its phosphoderivatives (VIP1\_A, lane 4; VIP1\_D, lane 5). Protoplast lysates were subjected to immunoprecipitation with rabbit antibody to Myc. Crude lysates (upper panel) and immunoprecipitated proteins (lower panel) were detected with mouse antibodies to HA and Myc. Cotransfection of MPK3-HA and its known interactor MKK4 (\*, Myc-tagged) served as a positive control (lane 1). **(C)** Schematic diagram of VIP1 protein. The MAPK phosphorylation site, Ser<sup>79</sup>, and bZIP domain are indicated. **(D)** In vitro kinase assay. MPK3 (lane 1) or activated MPK3 (lanes 2 to 4), which had been immunoprecipitated from protoplasts expressing MPK3-HA alone or in combination with its activator MKK4-Myc, respectively, were incubated with the following substrates: MBP (lanes 1 and 2, positive control), recombinant proteins GST (lane 3, negative control), or GST-VIP1 (lane 4). Autoradiography (upper panel) and Coomassie blue-stained SDS-polyacrylamide gel electrophoresis (CBB, lower panel) are shown.

treatment and further increased over time in the case of MPK3 and MPK6. These data show that *A. thaliana* recognizes agrobacteria and that this recognition triggers the activation of multiple MAPKs, including MPK3.

To investigate whether *Agrobacterium*-induced activation of MPK3 correlates with a relocalization of VIP1, estradiol-induced leaves of VIP1-YFP plants were treated with *Agrobacterium tumefaciens* and analyzed by confocal microscopy. Within 5 min of bacterial contact, wild-type VIP1-YFP accumulation was observed in leaf nuclei (Fig. 2C). Treatment with flg22 and agrobacteria triggered the aggregation of some VIP1-YFP as well as VIP1\_A-YFP in vesicle-like structures (Fig. 2, B and C, and fig. S2).

Because VIP1 rapidly relocalizes to the nucleus upon contact with agrobacteria or the flg22 peptide, we hypothesized that VIP1 plays a more general role in host defense response. One typical response of the pathogen-induced MAPK pathway is expression of the pathogenesis-related *PR1* gene (8). We therefore investigated the potential effect of enhanced nuclear VIP1 levels on *PR1* expression in protoplasts transfected with a *PR1* promoter-driven GUS construct (*PR1::GUS*) and VIP1-HA or *PR1::GUS* alone, respectively. Compared to protoplasts transfected with *PR1::GUS* only, GUS activity in protein extracts from protoplasts cotransfected with VIP1-HA and *PR1::GUS* was significantly enhanced (Fig. 3A). In order to verify

that the nuclear localization of VIP1 is essential for its function in biotic stress gene modulation, we tested the effect of a membrane-targeted myristoylated/palmitoylated Myr-VIP1-YFP fusion protein on *PR1* promoter-driven GUS expression in protoplasts. In contrast to VIP1-YFP, Myr-VIP1-YFP failed to induce *PR1::GUS* expression, confirming the functional relevance of the subcellular localization of VIP1 (Fig. 3A).

Because we observed *Agrobacterium*-triggered phosphorylation and nuclear translocation of VIP1, we then investigated whether the nuclear import of the VirE2/T-DNA complex (11) also relies on the phosphorylation of VIP1. To this end, *Arabidopsis* root cell

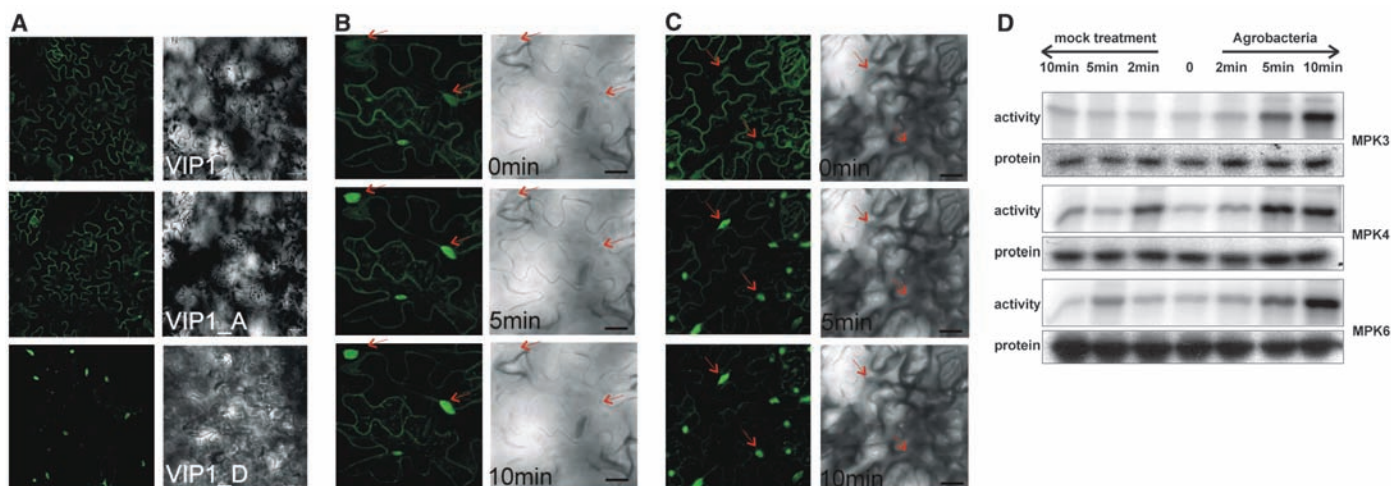
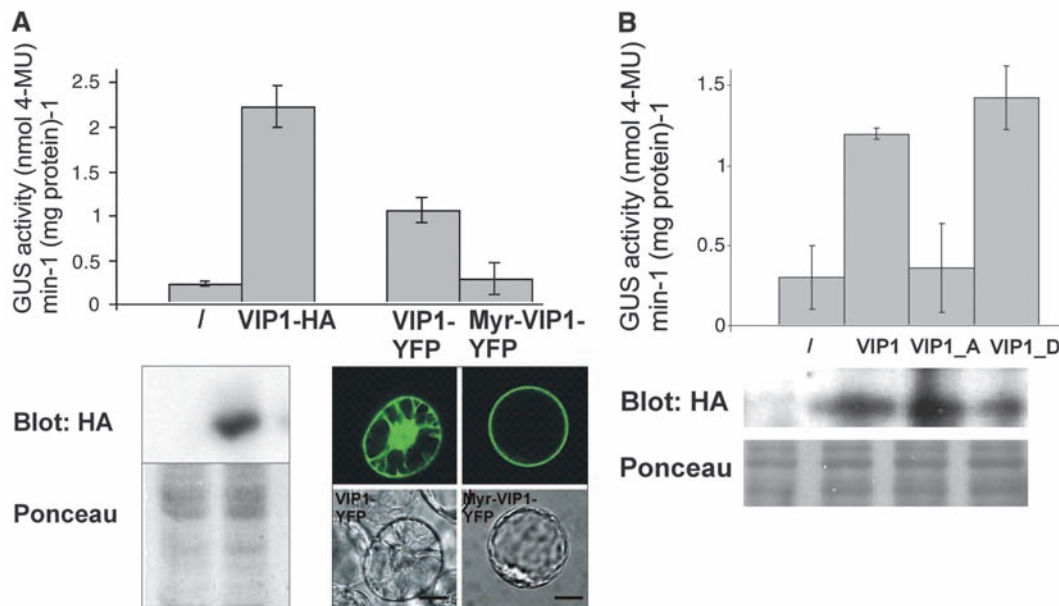


**Fig. 2.** Nuclear translocation of VIP1 is regulated by phosphorylation through stress-induced MPK3. (A to C) Confocal images of leaves from 5-week-old stable transgenic *A. thaliana* plants with estradiol-induced (40 μM for 12 hours) VIP1-YFP, VIP1\_A-YFP, or VIP1\_D-YFP expression. Left columns, YFP fluorescence; right columns, bright-field image. (B) VIP1 nuclear relocalization upon application of flagellin (1 μM) and (C) of an agrobacterial suspension. Scale bars,

20 μM. (D) *Agrobacterium*-induced MAPK activation. *A. thaliana* seedlings were treated with an agrobacterial suspension and harvested at the time points indicated. MAPKs were immunoprecipitated with specific antibodies, and their activity was monitored by *in vitro* kinase assays with the substrate MBP. The presence of equal amounts of the MAPK protein in each protein extract was confirmed by immunoblotting.

**Fig. 3.** (A) *PR1* induction by nuclear VIP1. GUS activity in protoplasts 16 hours after transfection with a *PR1* promoter::GUS construct alone or in combination with a VIP1-HA, VIP1-YFP, or Myr-VIP1-YFP construct is shown ( $n = 6$  independent protoplast transfection assays; error bars indicate SD). Expression of HA and YFP fusion proteins is visualized by immunoblotting and confocal microscopy, respectively. Scale bar, 20 μM. (B) VIP1 phosphorylation is required for nuclear import of agrobacterial T-DNA. GUS activity in cultured *Arabidopsis* root cells after 3 days of incubation with the agrobacterial virE3-deficient reporter strain (35S::GUSintron) and/or an effector strain (35S::VIP1-Myc, VIP1\_A-Myc, or VIP1\_D-Myc) is shown. A representative of four independent experiment series is shown ( $n = 3$  independent coincubation samples; error bars indicate SD). Lower panel: anti-Myc immunoblotted protein extracts.



cultures were incubated with an *Agrobacterium* reporter strain carrying a 35S::GUS construct and/or an effector strain carrying a 35S::VIP1-Myc, 35S::VIP1\_A-Myc, or 35S::VIP1\_D-Myc construct. Transformation efficiency was measured by quantitative GUS fluorescence after 3 days of incubation. Consistent with previous reports, *Agrobacterium* transformation efficiency increased greatly upon coexpression of VIP1 (Fig. 3B). However, this effect was observed only for wild-type VIP1 and VIP1\_D, but not VIP1\_A (Fig. 3B). The reason why constitutively nuclear-targeted VIP1\_D can enhance T-DNA transfer is most likely because the continuous protein synthesis of VIP1 enables the T-DNA complex to shuttle directly with de novo-synthesized cytosolic VIP1\_D to the nucleus. The possibility that the increased GUS activity in VIP1- and VIP1\_D-expressing cells was due to a transcriptional activation of the 35S promoter can be excluded, because GUS activity in protoplasts transfected with a 35S::GUS reporter was unaffected by cotransfection with VIP1, VIP1\_A, or VIP1\_D (fig. S3). Overall, these results confirm previous reports (6, 14) that the efficiency of *Agrobacterium* transformation can

be enhanced by coexpression of VIP1, but show that this effect depends on the ability to phosphorylate and thereby shuttle VIP1 into the nuclear compartment.

Our work suggests a role for VIP1 as a transcription factor in host defense, whose subcellular localization is regulated by an *Agrobacterium*-induced MAPK cascade. We hypothesize that at some point in evolution, agrobacteria took advantage of being recognized by the host by encroaching on VIP1 as a T-DNA shuttle into the host nucleus (fig. S4). Future research should allow the identification of the complete set of target genes regulated by VIP1 in the plant and help to unravel the role of VIP1 in transcriptional regulation during pathogen defense.

#### References and Notes

1. T. Nurnberger, F. Brunner, B. Kemmerling, L. Piater, *Immuno. Rev.* **198**, 249 (2004).
2. A. Espinosa, J. R. Alfano, *Cell. Microbiol.* **6**, 1027 (2004).
3. Z. Nimchuk, T. Eulgem, B. F. Holt 3rd, J. L. Dangl, *Annu. Rev. Genet.* **37**, 579 (2003).
4. D. A. Jones, D. Takemoto, *Curr. Opin. Immunol.* **16**, 48 (2004).
5. A. C. Vergunst *et al.*, *Science* **290**, 979 (2000).
6. V. Citovsky *et al.*, *Cell. Microbiol.* **9**, 9 (2007).

7. H. Nakagami, A. Pitzschke, H. Hirt, *Trends Plant Sci.* **10**, 339 (2005).
8. T. Asai *et al.*, *Nature* **415**, 977 (2002).
9. T. Meszaros *et al.*, *Plant J.* **48**, 485 (2006).
10. T. S. Nuhse, S. C. Peck, H. Hirt, T. Boller, *J. Biol. Chem.* **275**, 7521 (2000).
11. T. Tzfira, M. Vaidya, V. Citovsky, *EMBO J.* **20**, 3596 (2001).
12. R. Y. Ma *et al.*, *J. Cell Sci.* **118**, 795 (2005).
13. J. Li, A. Krichevsky, M. Vaidya, T. Tzfira, V. Citovsky, *Proc. Natl. Acad. Sci. U.S.A.* **102**, 5733 (2005).
14. T. Tzfira, M. Vaidya, V. Citovsky, *Proc. Natl. Acad. Sci. U.S.A.* **99**, 10435 (2002).
15. We thank E. Scheikl, M. Teige, A. Auer, S. Schwarz, and A. Belokurov for assistance and P. Guggenthaler for the introduction to the confocal microscope. We thank P. Hooykaas (Leiden University, Netherlands) for providing us with the virE3-deficient and wild-type agrobacterial strains LBA1010, and C. Zipfel (John Innes Center, Norwich, UK) for providing the 35S::GUSintron\_pBin construct. The work was supported by projects of the Austrian Science Fund FWF, the Vienna Science and Technology Fund, and the University of Vienna.

#### Supporting Online Material

www.sciencemag.org/cgi/content/full/318/5849/453/DC1  
Materials and Methods  
Figs. S1 to S4  
References

20 July 2007; accepted 29 August 2007  
10.1126/science.1148110

## Structure of a NHEJ Polymerase-Mediated DNA Synaptic Complex

Nigel C. Brissett,<sup>1\*</sup> Robert S. Pitcher,<sup>1\*</sup> Raquel Juarez,<sup>2</sup> Angel J. Picher,<sup>2</sup> Andrew J. Green,<sup>1</sup> Timothy R. Dafforn,<sup>3</sup> Gavin C. Fox,<sup>4</sup> Luis Blanco,<sup>2†</sup> Aidan J. Doherty<sup>1†</sup>

Nonhomologous end joining (NHEJ) is a critical DNA double-strand break (DSB) repair pathway required to maintain genome stability. Many prokaryotes possess a minimalist NHEJ apparatus required to repair DSBs during stationary phase, composed of two conserved core proteins, Ku and ligase D (LigD). The crystal structure of *Mycobacterium tuberculosis* polymerase domain of LigD mediating the synapsis of two noncomplementary DNA ends revealed a variety of interactions, including microhomology base pairing, mismatched and flipped-out bases, and 3' termini forming hairpin-like ends. Biochemical and biophysical studies confirmed that polymerase-induced end synapsis also occurs in solution. We propose that this DNA synaptic structure reflects an intermediate bridging stage of the NHEJ process, before end processing and ligation, with both the polymerase and the DNA sequence playing pivotal roles in determining the sequential order of synapsis and remodeling before end joining.

**D**NA double-strand breaks (DSBs) are a potentially lethal form of cellular damage, and failure to repair such breaks can lead to genomic instability (1, 2). In higher eukaryotes, the nonhomologous end joining (NHEJ) pathway is critical for the repair of DSBs (1). A

functionally homologous repair system exists in many prokaryotes, where it is used to repair DSBs in stationary-phase and sporulating cells (3, 4). The bacterial NHEJ complex is composed of two proteins, Ku and a multifunctional DNA ligase (LigD) (3–10). In addition to a core ligase domain, LigD often possesses ancillary polymerase (PolDom) and nuclease domains (6–15). PolDom, a member of the archaeo-eukaryotic primase (AEP) superfamily (6, 16, 17), in turn has a variety of nucleotidyl transferase activities (6–9) as well as the ability to generate template distortions and primer realignment (12, 13). Here, we describe the crystal structure of a NHEJ polymerase-mediated synaptic complex, which reveals a DNA-directed

mechanism used by repair polymerases to induce synapsis of noncomplementary ends through a dimeric arrangement.

PolDom can interact with a 3'-protruding DNA end containing a 5'-phosphate (5'-P) on the downstream strand (12), a probable first step in end joining, which is compatible with Ku binding near the ends. In the second step, PolDom may endeavor to connect the 3'-protruding DNA ends to configure a "gap-like" synaptic intermediate. When different DNA molecules were tested in polymerization assays, extension of the 3'-protruding strand by the *Mycobacterium tuberculosis* polymerase domain (Mt-PolDom) of LigD was observed by providing nucleoside triphosphates. However, template extension was restricted to the addition of a few nucleotides, suggesting that the specific nucleotides inserted may be templated, perhaps as a result of the pairing of the 3' ends. In the DNA shown in Fig. 1A, the 3'-protruding nucleotide [deoxycytidine (dC)] is complementary to the base preceding the nucleotide (dC), which is adjacent to the 5'-P; therefore, a structure resembling a single-nucleotide gap can be formed, either by self-annealing (snap-back) or by connection of two ends (synapsis). In agreement with this mechanism, guanosine triphosphate (GTP) was preferentially incorporated by PolDom.

The specificity of the elongation reaction was analyzed using variants of the 3'-protruding oligonucleotide that differed in the deoxynucleotide (X) adjacent to the internal 5'-P. As predicted, the base preferentially added to the 3'-protruding strand varied as a function of the X nucleotide, which acts as a template (fig. S1). Having shown

<sup>1</sup>Genome Damage and Stability Centre, University of Sussex, Brighton BN1 9RQ, UK. <sup>2</sup>Centro de Biología Molecular Severo Ochoa, CSIC-UAM, 28049 Madrid, Spain. <sup>3</sup>Department of Biosciences, University of Birmingham, Birmingham B15 2TT, UK. <sup>4</sup>European Synchrotron Radiation Facility, LL5-BM16, Grenoble Cedex 9, France.

\*These authors contributed equally to this work.

†To whom correspondence should be addressed. E-mail: lblanco@cbm.uam.es (L.B.); ajd21@sussex.ac.uk (A.J.D.)